

1-1-1997

Efficient Wavelength Shifting Over The Erbium Amplifier Bandwidth Via Cascaded Second Order Processes In Lithium Niobate Waveguides

Katia Gallo

Gaetano Assanto

George I. Stegeman
University of Central Florida

Find similar works at: <https://stars.library.ucf.edu/facultybib1990>
University of Central Florida Libraries <http://library.ucf.edu>

This Article is brought to you for free and open access by the Faculty Bibliography at STARS. It has been accepted for inclusion in Faculty Bibliography 1990s by an authorized administrator of STARS. For more information, please contact STARS@ucf.edu.

Recommended Citation

Gallo, Katia; Assanto, Gaetano; and Stegeman, George I., "Efficient Wavelength Shifting Over The Erbium Amplifier Bandwidth Via Cascaded Second Order Processes In Lithium Niobate Waveguides" (1997). *Faculty Bibliography 1990s*. 1917.
<https://stars.library.ucf.edu/facultybib1990/1917>

Efficient wavelength shifting over the erbium amplifier bandwidth via cascaded second order processes in lithium niobate waveguides

Cite as: Appl. Phys. Lett. **71**, 1020 (1997); <https://doi.org/10.1063/1.119714>

Submitted: 05 March 1997 . Accepted: 23 June 1997 . Published Online: 04 June 1998

Katia Gallo, Gaetano Assanto, and George I. Stegeman



View Online



Export Citation

ARTICLES YOU MAY BE INTERESTED IN

[First-order quasi-phase matched LiNbO₃ waveguide periodically poled by applying an external field for efficient blue second-harmonic generation](#)

Applied Physics Letters **62**, 435 (1993); <https://doi.org/10.1063/1.108925>

[1.5 μm band efficient broadband wavelength conversion by difference frequency generation in a periodically domain-inverted LiNbO₃ channel waveguide](#)

Applied Physics Letters **63**, 3559 (1993); <https://doi.org/10.1063/1.110096>

[Periodic domain inversion in x-cut single-crystal lithium niobate thin film](#)

Applied Physics Letters **108**, 152902 (2016); <https://doi.org/10.1063/1.4946010>



Measure Ready
M91 FastHall™ Controller

A revolutionary new instrument for complete Hall analysis

[See the video](#)

Lake Shore
CRYOTRONICS

Efficient wavelength shifting over the erbium amplifier bandwidth via cascaded second order processes in lithium niobate waveguides

Katia Gallo and Gaetano Assanto^{a)}

Department of Electronic Engineering, Terza University of Rome, Via della Vasca Navale 84, 00146 Rome, Italy

George I. Stegeman

CREOL University of Central Florida, Orlando, Florida 32816-2700

(Received 5 March 1997; accepted for publication 23 June 1997)

We investigate two schemes for wavelength conversion based on the cascading of two successive second order processes in a quasi-phase-matched lithium niobate channel waveguide. Efficient conversion over the full erbium amplifier bandwidth is possible with a single multi-hundred milliwatt pump laser operating around 1.55 μm . © 1997 American Institute of Physics. [S0003-6951(97)01834-2]

Efficient wavelength conversion of very high bit rate signals is a key issue in wavelength division multiplexing (WDM) networks. The most widely investigated conversion techniques have utilized semiconductor amplifiers either for four-wave mixing or modulation of the saturated gain.^{1,2} A number of issues such as very limited 3 dB bandwidth, cross talk, insertion loss, amplifier noise, etc. make this a nonideal solution and there is a continuing search for other approaches. Among them, those exploiting nonlinear optical wave mixing via second order nonlinearities appear promising because they also provide spectral inversion with the addition of low excess noise.³ In fact, wavelength shifting of signals has been demonstrated via difference frequency generation (DFG) in quasi-phase-matched (QPM) lithium niobate (LN=LiNbO₃) with a pump laser operating in the wavelength range of 750–800 nm.^{4,5} Although successful, this particular approach is problematic because the waveguides are typically multimode for input in the near-infrared and require lasers outside of the communications bands. Here we describe an approach which also relies on DFG, but which is based on cascading of second harmonic generation (SHG) of a pump laser in the communications band and then DFG, both in the same channel waveguide.

Cascading of second order processes has been shown to encompass new exciting possibilities for all-optical signal processing.⁶ From the early days of nonlinear optics it is known that $\chi^{(2)}:\chi^{(2)}$ processes could mimic four-wave-mixing in a noncentrosymmetric material. In the 1980's Baranova and Zel'dovich predicted large efficiencies for SHG via $\chi^{(2)}(-2\omega;\omega;\omega)$ followed by DFG via $\chi^{(2)}(-\omega_3;2\omega,-\omega_2)$ taking place in a noncentrosymmetric nonlinear medium.⁷ This phenomenon has been experimentally observed for wavelengths around 1064 nm in bulk β -barium borate by Tan *et al.*⁸ and has interesting implications for wavelength shifting devices: the SHG from a strong input wave at ω interacting with a weak input signal at $\omega_2 = \omega - \delta\omega$ (with $\delta\omega \ll \omega$) can generate an output signal at $\omega_3 = 2\omega - \omega_2 = \omega + \delta\omega$. The wavelength shifter proposed here operates with inputs around 1.55 μm , an appealing feature for WDM networks where high quality lasers have been

developed specifically for communications. The chosen guided-wave geometry in QPM lithium niobate leads to multi-hundred milliwatt operating powers. In this letter we report on numerical investigations of two simple configurations, and evaluation of the device performance in terms of signal attenuation/gain and bandwidth.

Simulations were performed for the different field polarizations allowed by the tensorial structure of the LN nonlinear susceptibility for SHG at wavelengths in the fiber communication spectral window at $\lambda_p = 1.55 \mu\text{m}$ (input pump), $\lambda_2 = \lambda_p + \delta\lambda$ (input signal), $\lambda_3 = 1/(2/\lambda_p - 1/\lambda_2)$ (frequency shifted signal through DFG) with $\delta\lambda|_{\text{max}} = \pm 50 \text{ nm}$. It was found that an efficient implementation of the cascaded interaction requires the fields at λ_2 , λ_3 , and $\lambda_p/2$ to be collinear because this prevents the DFG wave vector mismatch from varying appreciably when tuning the input signal around 1.55 μm .

The device proposed here is readily available, an annealed proton exchanged (APE) channel waveguide in a Z-cut LN crystal, supporting only X-propagating quasi-TM₀₀ modes at 1.55 μm . The transverse refractive index profile is taken to be: $n(y,z) = n_e + \Delta n_e \exp(-|z|/d) \exp(-|y|/w)$, with n_e given by standard Sellmeier equations.⁹ The effective index method with a finite difference algorithm was employed to calculate the transverse field profiles and their wave vectors along the propagation direction for each mode of the structure. For typical parameters $\Delta n_e = 0.025$, $T = 300 \text{ K}$,

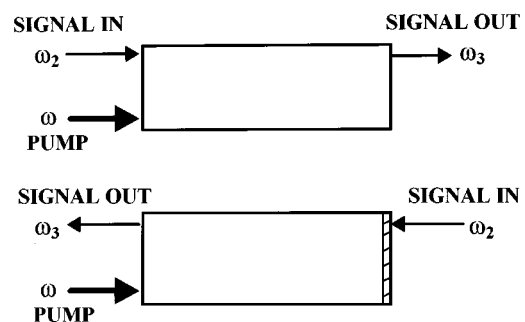


FIG. 1. Sketch of the device in two simple configurations: (a) copropagating pump and signal; (b) counterpropagating pump and signal, with a coated endface, reflecting at $\lambda_p/2$ and transmitting at λ_p .

^{a)}Electronic mail: assanto@ele.uniroma3.it

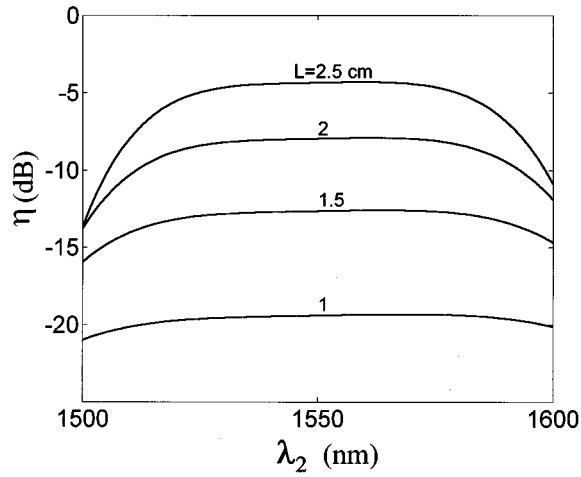


FIG. 2. cw response of the single pass device [Fig. 1(a)] vs signal wavelength for various waveguide lengths L . The vertical axes are the conversion efficiencies in dB. Here $P_{\text{signal}}=1$ mW and $P_{\text{pump}}=300$ mW.

$d=2\ \mu\text{m}$, $w=3\ \mu\text{m}$, the waveguide is single moded at $\lambda_p\ \lambda_2\ \lambda_3$, while several modes ($\text{TM}_{00}, \text{TM}_{01}, \text{TM}_{10}$) are supported at the second harmonic ($\lambda_p/2$). First order quasi-phase matching (QPM) through ferroelectric domain inversion with period $\Lambda=16.7\ \mu\text{m}$ is then required for efficient SHG from λ_p . Under these conditions only the following interactions are significant inside the structure: $\text{TM}_{00}(\lambda_p) + \text{TM}_{00}(\lambda_p) \rightarrow \text{TM}_{00}(\lambda_p/2)$ and $\text{TM}_{00}(\lambda_p/2) - \text{TM}_{00}(\lambda_2) \leftrightarrow \text{TM}_{00}(\lambda_3)$; the others being negligible because of their large wave vector mismatch or small overlap integrals. While the first interaction indicates a pumping mechanism to upconvert the input frequency, in the second the double arrow points out the presence of a slight mismatch which occurs as wavelength is scanned over the Er^+ amplifier bandwidth.

The modeling of the interactions utilizes the standard coupled mode theory for waveguides. In the lossless case, this leads to the coupled mode equations in the slowly varying envelope approximation:

$$\frac{dA_1}{dx} = -iK_{11}BA_1^* \exp(-i\Delta\beta_1x),$$

$$\frac{dA_2}{dx} = -i(\lambda_p/\lambda_2)K_{23}BA_3^* \exp(-i\Delta\beta_2x),$$

$$\frac{dA_3}{dx} = -i(\lambda_p/\lambda_3)K_{23}BA_2^* \exp(-i\Delta\beta_2x),$$

$$\frac{dB}{dx} = -iK_{11}A_1^2 \exp(i\Delta\beta_1x) - 2iK_{23}A_2A_3 \exp(i\Delta\beta_2x),$$

where A_1 , A_2 , A_3 , and B are the field amplitudes at $\lambda_p, \lambda_2, \lambda_3, \lambda_p/2$, respectively; $\Delta\beta_1=4\pi[(N_{\text{SH}}-N_1)/\lambda_p] - 2\pi/\Lambda$ and $\Delta\beta_2=2\pi(2N_{\text{SH}}/\lambda_p - N_2/\lambda_2 - N_3/\lambda_3) - 2\pi/\Lambda$ are the SHG and DFG wave vector mismatches (with N indicating the effective guided mode indices), and the two nonlinear coupling coefficients are:

$$K_{i,j} = \frac{2\pi}{\lambda_p} \sqrt{\frac{2c\mu_0}{S_{ij}}} \frac{d_{\text{eff}}}{\sqrt{N_i N_j N_{sh}}}$$

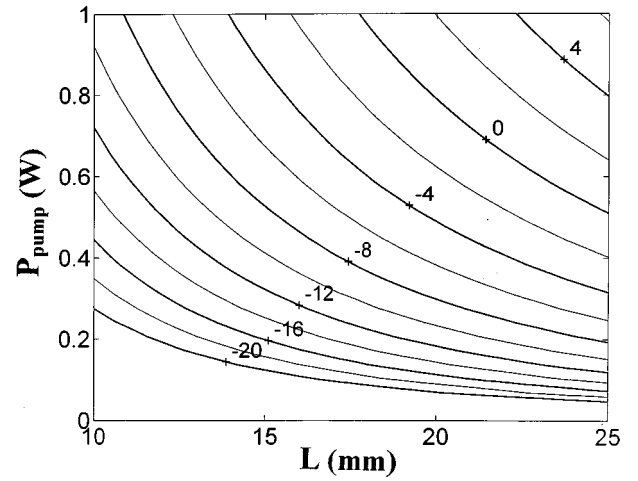


FIG. 3. Contour map response of the single pass device [Fig. 1(a)] vs waveguide length L and pump power P_{pump} . The lines are marked with the corresponding conversion efficiencies in dB.

with $(i,j)=(1,1)$ or $(2,3)$, if Kleinman symmetry holds. For λ_2 (signal) ranging from 1.5 to 1.6 μm , we found effective channel waveguide cross sections $S_{23} \cong S_{11} \cong 49.5\ \mu\text{m}^2$, in agreement with values obtained through more accurate index profile modeling.¹⁰ For the nonlinear strength, the measured value of $d_{33}=27\ \text{pm/V}$ in a uniform, depth-independent QPM grating obtained via electric-field poling was used.¹¹ It yields $d_{\text{eff}}=(2/\pi)d_{33}$ and $K_{23} \cong K_{11} \cong 0.086[\text{W}^{1/2}\ \text{mm}^{-1}]$, corresponding to a normalized SHG conversion efficiency of $\eta_{\text{nor}}=74\%[\text{W}^{-1}\ \text{cm}^{-2}]$, which compares well with reported experimental values of 43% $[\text{W}^{-1}\ \text{cm}^{-2}]$ that include propagation losses.¹²

Let us first consider the case [Fig. 1(a)] of both signal and pump inputs entering the crystal from the same side. For $\lambda_p=1.55\ \mu\text{m}$, $\lambda_3=\lambda_2+\delta\lambda$ and $\Delta\beta_1=0$ (i.e., perfectly phase matched SHG), Fig. 2 shows the $\lambda_2 \rightarrow \lambda_3$ conversion efficiency with cw inputs versus λ_2 . Notice the broad conversion bandwidth, comparable with DFG processes in the near IR with QPM-LN.¹³ Signal amplification, due to the

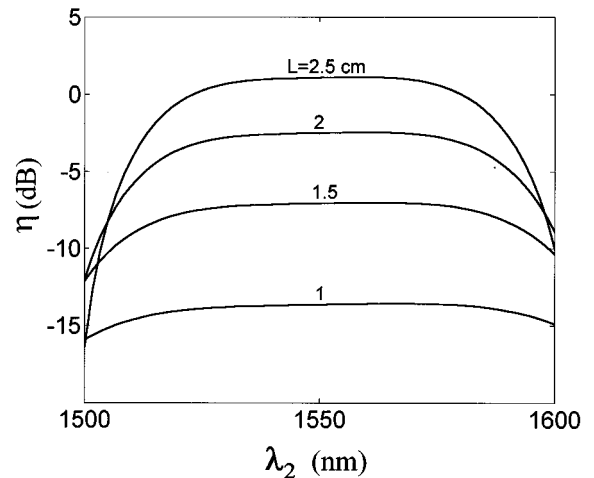


FIG. 4. Response of the two-pass device [Fig. 1(b)] vs signal wavelength for various L . The vertical axis is the conversion efficiency in dB, which clearly shows an enhancement compared to the case in Fig. 2. Here $P_{\text{signal}}=1$ mW and $P_{\text{pump}}=300$ mW.

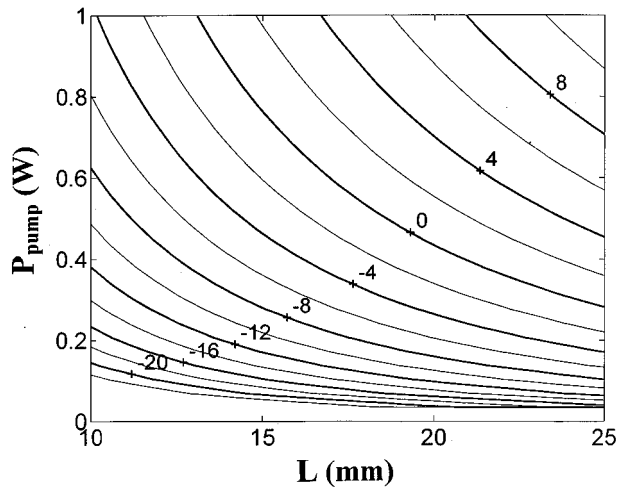


FIG. 5. Contour map response of the two-pass device [Fig. 1(b)] vs L and pump power. The lines are marked with the resulting conversion efficiencies in dB, and in this case also show the enhancement afforded by the counter-propagating configuration.

parametric nature of the interaction, is obtained by increasing the crystal length and/or the pump power at $\lambda = 1.55 \mu\text{m}$. Both parameters affect the conversion efficiency, as shown in Fig. 3 for input at $\lambda_2 = 1.55 \mu\text{m} + 20 \text{ nm}$ and for a signal power of 1 mW. The lines are marked by the signal gain in dB. The simulations have confirmed that the output signal power, due to the cascading of SHG and DFG, increases linearly with the signal power, quadratically with the pump power and varies as L^a (with $3 < a < 4$) for pump powers below 1 W.

The simple geometry of Fig. 1(a) can be modified with the addition of a $\lambda_p/2$ reflective coating in order to maximize the SHG prior to DFG, as sketched in Fig. 1(b). The pump, injected through the uncoated endface, is partially converted to the SH on the first pass through the crystal and then leaves it. The SH wave at $\lambda_p/2$ is reflected and interacts through DFG with the signal launched from the opposite (to the λ_p launching) side. We assumed 100% reflectivity at $\lambda_p/2$. Highly transmitting coatings at λ_p are preferable to eliminate the pump wavelength at the device output. As is intuitively clear, the more of the second harmonic generated in the first pass, the greater the advantage in adopting this latter scheme. Figures 4 and 5 are the counterparts of Figs. 2 and 3 calcu-

lated for the same input conditions. The device still exhibits a wide conversion bandwidth typical of the DFG process, which compares favorably with other techniques for wavelength shifting and with the possibility of signal amplification at higher pump excitation.

In conclusion, single- and double-pass configurations for a broadband, and integrated wavelength shifter for WDM in a lithium niobate quasi-phase-matched channel waveguide have been analyzed numerically. The wavelength converters operate in the $1.55 \mu\text{m}$ spectral window for optical fiber communications and require reasonable pump powers and propagation lengths to provide lossless, or even amplified wavelength conversion. The adoption of a contradirectional geometry for the signal and pump further improves the predicted performance, and offers a simple method for removing the pump beam. We are confident that this novel element for WDM communications, which is well within reach of today's technological capabilities, might become one of the first practical devices based on nonlinear cascading.

The work in Italy was supported by the National Research Council (Grants 96.02238.CT07 and 96.02514.CT07) and in the USA by DARPA.

- ¹J. Zhou, N. Park, K. J. Vahala, M. A. Newkirk, and B. I. Miller, *Electron. Lett.* **30**, 859 (1994); W. Shieh, E. Park, and A. E. Willner, *IEEE Photonics Technol. Lett.* **8**, 524 (1996).
- ²R. J. Manning and D. A. O. Davies, *Opt. Lett.* **19**, 889 (1994); T. Durhuus, B. Mikkelsen, C. Joergensen, S. Lykke Danielson, and K. E. Stubkjaer, *J. Lightwave Technol.* **14**, 942 (1996).
- ³S. J. B. Yoo, *J. Lightwave Technol.* **14**, 955 (1996).
- ⁴C. Q. Xu, H. Okayama, K. Shinozaki, K. Watanabe, and M. Kawahara, *Appl. Phys. Lett.* **63**, 1170 (1993); C. Q. Xu, H. Okayama, and M. Kawahara, *Appl. Phys. Lett.* **63**, 3559 (1993).
- ⁵M. L. Bortz, D. Serkland, and M. M. Fejer, *Technical Digest of the CLEO'94 Meeting* (Optical Society of America, Washington, DC, 1994), pp. 288–289.
- ⁶G. I. Stegeman, R. Schiek, L. Torner, W. Torruellas, Y. Baek, D. Baboiu, Z. Wang, E. Van Stryland, D. Hagan, and G. Assanto, in *Novel Optical Materials and Applications*, edited by I. C. Khoo, F. Simoni, and C. Umeton (Wiley, New York, 1997), pp. 49–76.
- ⁷N. B. Baranova and B. Ya. Zel'dovitch, *Sov. Phys. Dokl.* **27**, 222 (1982); *Dokl. Akad. Nauk SSSR* **263**, 325 (1982).
- ⁸H. Tan, G. P. Banfi, and A. Tomaselli, *Appl. Phys. Lett.* **63**, 2472 (1993).
- ⁹D. F. Nelson and R. Mikulyak, *J. Appl. Phys.* **45**, 3698 (1974).
- ¹⁰M. L. Bortz, Ph.D. dissertation, Stanford University, 1994.
- ¹¹K. Kintaka, M. Fujimura, T. Suhara, and H. Nishihara, *J. Lightwave Technol.* **14**, 462 (1996).
- ¹²M. A. Arbore and M. M. Fejer, *Opt. Lett.* **22**, 151 (1997).
- ¹³C. Q. Xu, H. Okayama, and T. Kamijoh, *Jpn. J. Appl. Phys.* **34**, 1543 (1995).